Journal of Soils and Sediments
https://doi.org/10.1007/s11368-020-02756-3

SOILS, SEC 2 • GLOBAL CHANGE, ENVIRON RISK ASSESS, SUSTAINABLE LAND USE • RESEARCH ARTICLE

Quantitative analysis of driving factors in soil erosion using geographic detectors in Qiantang River catchment, Southeast China

Shizhengxiong Liang [1,2] · Haiyan Fang [1,2]

Received: 13 August 2019 / Accepted: 13 August 2020

Abstract

Purpose Soil erosion has received enormous attention from the scientific community and government across the world. This study aims to detect those important driving factors and their potential interactions on soil erosion. Findings would facilitate the rational development of soil and water conservation.

Materials and methods Here, soil erosion was simulated using the Revised Universal Soil Loss Equation (RUSLE) in the Qiantang River catchment, southeast China, for the period of 2006–2015. Contributions to soil erosion by six driving factors including land cover type, annual rainfall, elevation, slope, soil type, and vegetation coverage were quantitatively analyzed via Qiantang River Catchment geographic detectors.

Results and discussions The results suggest that vegetation coverage explains 7.28% of soil erosion distribution, and the impact of vegetation coverage on soil erosion is significantly larger than that of the other five driving factors ($p < 0.05$). In recent years, the explanatory power of vegetation coverage to soil erosion has experienced a change from increasing to decreasing trend. The interaction between vegetation coverage and slope explains up to 32.69% of soil erosion distribution, and an increasing trend has been detected in the explanatory power of this interaction. The spatial heterogeneity of soil erosion can be well understood by vegetation coverage and elevation. The high-risk areas are featured by elevation ranging from 1135 to 1777 m or vegetation coverage between 50 and 62%. Changes in vegetation coverage and its spatial distribution at different elevations are the main causes of the variations in the explanatory power.

Conclusions The spatial analysis and quantitative analysis of six driving factors in soil erosion have improved the understanding of the heterogeneity in soil erosion. Measures in soil and water conservation should be strengthened in high-risk areas. The interaction between vegetation coverage and slope is the dominating contributor to soil erosion. The study provides a scientific basis for rational prevention of soil erosion in the Qiantang River catchment.

Keywords Qiantang River catchment · RUSLE · Soil erosion · Geographic detectors · Driving factors

1 Introduction

Soil erosion, one of the top risky environmental issues across the world, has been an important research topic for scientific researchers (Borrelli et al. 2017). Like other environmental problems, such as the decline of agriculture productivity, river siltation, riverbed elevation, and water pollution (Lal 1998), soil erosion can seriously threaten the sustainable development of both nature and society. Soil erosion can be influenced by many factors including rainfall, runoff, vegetation, landform, anthropogenic activities, and soil anti-erosion system (Wei et al. 2012). Therefore, to further implement measures in soil and water conservation, it is of great significance to quantify the substantial contributions to soil erosion by different driving factors as well as their interactions.

Extensive work has been conducted to identify the driving factors of soil erosion in previous studies (El Kateb et al. 2013; Sun et al. 2014; Yu et al. 2019). Rainfall simulation experiments

Editorial Responsibility: Saskia D. Keesstra

✉ Haiyan Fang
fanghy@igsnrr.ac.cn

[1] Key Laboratory of Water Cycle and Related Land Surface Processes, Institute of Geographic Sciences and Natural Resources Research, Chinese Academy of Sciences, Beijing 100101, China

[2] College of Resources and Environment, University of Chinese Academy of Sciences, Beijing 100049, China

Published online: 22 August 2020

(Mhaske et al. 2019) and runoff plot monitoring (Xu et al. 2016) have been used on the slope scale to investigate the driving factors of soil erosion. Khan et al. (2016) assessed the effect of different simulated rainfall intensities with different slopes on soil erosion. However, it is not reliable to extrapolate the results on the slope scale directly to a watershed scale. On the other hand, most existing studies have applied traditional statistical methods such as correlation analysis or regression analysis to detect these driving factors (Shi et al. 2013; Feng et al. 2018; Golosov et al. 2018). For example, Chen et al. (2014) analyzed the spatial pattern of soil erosion and its relationship with different driving factors on the watershed scale. However, few studies shed light on the impact of interactions among different driving factors, especially the quantitative contributions of these interactions to soil erosion. Meanwhile, the spatial heterogeneity of soil erosion is barely clear. Future efforts are still needed to answer the above questions.

Geographic detectors are a set of statistical methods to detect spatial heterogeneity and reveal potential driving forces (Wang et al. 2010). It can analyze spatial heterogeneity, detect any relationship between two independent variables, quantify their relative contributions to dependent variables, and provide the interaction results. This approach has been widely used in social and natural sciences (Yang et al. 2016; Ren et al. 2016), but seldom in soil erosion studies with an exceptional work by Gao and Wang et al. (2018).

In the hilly regions of South China, the uneven distribution of rainfall amount and intensity, strong weathering, rapid social and economic development, and high population density have triggered severe soil erosion. Despite the wide-spread forest coverage in some regions, soil erosion can still be a serious issue (Zhu et al. 2013). Due to the thin soil layer, the severity of soil erosion in these regions is just inferior to that in the Loess Plateau (Liang et al. 2008; Ministry of Water Resources of China 2010). The Qiantang River catchment (QTC) in Zhejiang province is the most important freshwater resources. In recent years, the stochastic rainfall events and the combined effects of soil, topography, and land use resulted in a higher risk of soil erosion in this catchment (Wei et al. 2009; Rao et al. 2014). Because the natural and anthropogenic factors of this catchment are similar to those in South China, the QTC is thus a representative hilly catchment in South China.

Modeling is an efficient method to study soil erosion (Siswanto and Francés 2019). Process-based models are complex and require substantial data, which usually preclude their broad application. In contrast, a simple, physically plausible empirical model such as the Revised Universal Soil Loss Equation (RUSLE) is usually welcome, especially at regional and/or global scales (Borrelli et al. 2018).

Therefore, The QTC in Zhejiang province was selected in this study, and soil erosion rate of the QTC was first estimated by RUSLE, and then the geographic detectors were applied to quantify the contributions of each driving factor and their interactions to catchment soil loss. In this study, the driving factors vegetation coverage, land cover type, elevation, slope, rainfall, and soil type were selected in that they are the main factors influencing soil erosion and widely used in soil erosion studies (Shi et al. 2013; Yu et al. 2019).

2 Materials and methods

2.1 Study area

QTC (28° 00′ − 30° N, 117° 30′ − 120° 30′ E) is located in northwestern Zhejiang Province, Southeast China (Fig. 1). Dominated by a subtropical monsoon climate, annual rainfall in QTC varies from 1300 to 2300 mm from 2006 to 2015, mainly happens in June and July. Annual average temperature is around 17 °C, with the highest temperature record of 41 °C.

The slope in QTC ranges from 0 to 73.36° with an average slope gradient of 18.7°. Mountains and hills account for over 70% of the total catchment area, and red sandstones with a friable and easily eroded lithology dominate the hilly area. Major soil types include humicacrisols, haplicalisols, and dystricregosols. Forest, mostly distributed in mountainous areas, is the primary land cover type with a proportion of 70% of the total area whereas dry land and paddy fields mainly distribute in flat areas.

2.2 Data

To simulate soil erosion, elevation from the Digital Elevation Model with a spatial resolution of 30 m was retrieved from the geospatial data cloud platform of the Computer Network Information Center of the Chinese Academy of Sciences (http://www.gscloud.cn). TM land cover type with a 30-m spatial resolution in 2005, 2010, and 2015 were derived from the National Earth System Science Data Sharing Service Platform (http://www.geodata.cn). Furthermore, the soil type data with a scale of 1: 1,000,000 was obtained from the Resources and Environment Sciences of the Chinese Academy of Sciences (CAS) with soil attributes including clay, silt, sand, and organic carbon content checked from China Soil Species Database. Meanwhile, rainfall data were collected from the "Hydrological Yearbook of the People's Republic of China". The Moderate-resolution Imaging Spectroradiometer (MODIS) 16-d maximum Normalized Difference Vegetation Index (NDVI) with a spatial resolution (250 m) were collected during 2006–2015.

2.3 Methods

2.3.1 The RUSLE model

RUSLE, a widely used model in calculating the amount of soil erosion (Kinnell 2010), was applied to conduct

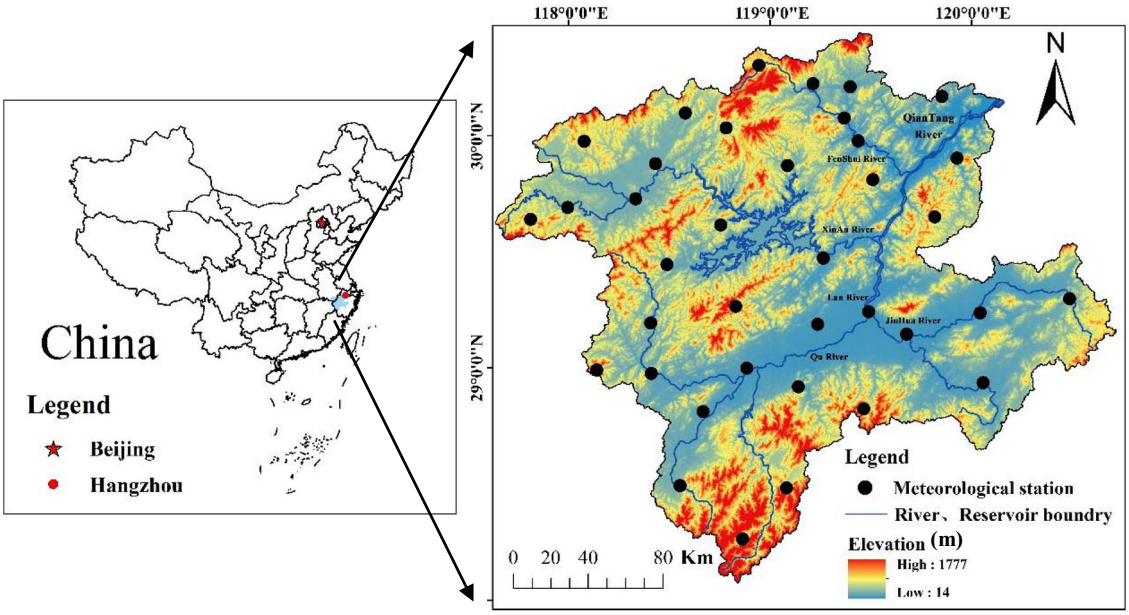

Fig. 1 Location of the study area and meteorological stations

the simulation experiments of soil erosion in QTC, which is shown as in Eq. 1.

$$A = R \times K \times L \times S \times C \times P \tag{1}$$

where, A is the average annual soil loss (t km^{-2} year^{-1}); R is the factor of rainfall erosivity (MJ mm ha^{-1} h^{-1} year^{-1}); K is the factor of soil erodibility (t hm^2 h hm^{-2} MJ^{-1} mm^{-1}); L, S are slope length and gradient (−); C is the factor of vegetation and management (−); P is the factor of soil and water conservation measures (−).

(1) Rainfall erosivity factor (R)

Rainfall erosivity (R) represents the external driving force of soil erosion. Rainfall parameters, including rainfall intensity, daily, monthly, and yearly rainfall amounts, are often used to estimate R (Cai et al. 2000). Zhou et al. (1995) proposed a method for estimating R in Fujian Province based on monthly rainfall amount. Zhang and Fu (2003) pointed out that R calculated by monthly rainfall data was accurate in the southern region. Given the fact that the climate, topography, and environmental conditions in Fujian Province is similar to those in our study area, the method (Eq. 2) proposed by Zhou et al. (1995) was adopted in this study.

$$R = \sum_{i=1}^{12}(-1.5527 + 0.1792P_i) \tag{2}$$

where R is the rainfall erosivity (MJ mm ha^{-1} h^{-1} year^{-1}), and P_i is the rainfall amount (mm) in month i.

(2) Soil erodibility factor (K)

K is a parameter used to characterize the sensitivity and resistance of soil to erosion. The method developed by Sharpley and Williams (1990) for estimating K in the Erosion-Productivity Impact Calculator (EPIC) model has been validated by Zheng et al. (2010) in hilly areas by observing 15 runoff plots for five consecutive years. Therefore, the method (Eq. 3) in EPIC was applied to calculate K.

$$K = 0.2 + 0.3e^{[-0.0256\mathrm{SAN}(1-\mathrm{SIL}/100)]} \times \left(\frac{\mathrm{SIL}}{\mathrm{CLA}+\mathrm{SIL}}\right)^{0.3} \times \left[1-\frac{0.25C}{C+e^{(3.27-2.95C)}}\right] \times \left[1-\frac{0.72SN}{\mathrm{SN}+e^{(22.9\mathrm{SN}-5.51)}}\right] \tag{3}$$

where, K is the soil erodibility factor (t hm^2 h hm^{-2} MJ^{-1} mm^{-1}); CLA, SIL, and SAN are clay, silt and sand content (%), respectively; C is organic carbon content (%), and SN = 1 − SAN/100.

(3) Topographic factor (L, S)

Slope length factor (L) and slope factor (S) indicate the impact of different landforms on soil erosion. L and S are usually extracted based on DEM on a watershed scale. Given the steep catchment slope, L and S were estimated using the methods proposed by Liu et al. (1994) and Liu et al. (2000) (Eqs. 4 and 5).

$$S = \begin{cases} 10.8\sin\theta + 0.03 & \theta \le 5° \\ 16.8\sin\theta - 0.05 & 5° < \theta < 10° \\ 21.9\sin\theta - 0.96 & \theta \ge 10° \end{cases} \tag{4}$$

$$L = (\lambda/22.1)^m, m = \begin{cases} 0.2 & \text{if } \theta \le 1° \\ 0.3 & \text{if } 1° < \theta \le 3° \\ 0.4 & \text{if } 3° < \theta \le 5° \\ 0.5 & \text{if } \theta > 5° \end{cases} \tag{5}$$

where, λ is slope length (m) and θ is the slope (degree). According to the D8 single-direction algorithm, the

cumulative slope length was calculated using the method proposed by van Remortel (2001), and then obtained L and S.

(4) Vegetation management factor (C)

Management factor (C) reflects the comprehensive effect of crop management and vegetation coverage. It is highly related to vegetation coverage and land cover type. Therefore, based on the MODIS NDVI data, the annual average vegetation coverage in the study area was extracted by classical pixel dichotomy model, and then C was calculated using the method by Cai et al. (2000) (Eq. 6).

$$C = \begin{cases} 1 & fc = 0 \\ 0.6508 - 0.3436 \cdot \lg(fc) & 0 < fc < 78.3\% \\ 0 & c \geq 78.3\% \end{cases} \quad (6)$$

where, fc is vegetation coverage (%), and C is the crop management factor (dimensionless).

(5) Soil and water conservation factor (P)

P refers to the ratio of soil loss after taking measures of soil and water conservation to that of downhill planting. P values of different land cover types in the study area were obtained based on previous studies (Huang et al. 2004; Chen et al. 2014; Jiang et al. 2014; Zha et al. 2015) (Table 1).

The spatial distribution of each factor in RUSLE is shown in Fig. 2.

2.3.2 Geographic detectors

The q value of geographic detectors can clearly quantify any relationships between the independent and dependent variables (Wang and Xu 2017). Four sub-detectors are included:

(1) Factor detector: It can detect the spatial heterogeneity of the dependent variable (Y) and the explanatory power of the independent variable (X). The explanatory power, defined by q ($0 < q < 1$), indicates that X can explain $q \times 100\%$ of the spatial heterogeneity of Y (Eqs. 7 and 8). Here, factor detector indicated the explanatory power of soil erosion by six driving factors and their interactions.

$$q = 1 - \frac{\sum_{h=1}^{L} N_h \sigma_h^2}{N\sigma^2} = 1 - \frac{SSW}{SST} \quad (7)$$

$$SSW = \sum_{h=1}^{L} N_h \sigma_h^2 SST = N\sigma^2 \quad (8)$$

where, h is the stratification (classification or partition) of the dependent variable Y or the independent variable X; N_h and N are the units of layer h and region; ${\sigma_h}^2$ and σ^2 are the variances of layer h and region, respectively; SSW and SST are the sum of intra-layer variances and the total variances of region, respectively; q can be transformed to the non-central F distribution and tested for significance.

$$F = \frac{N-L}{L-1} \frac{q}{1-q} \sim F(L-1, N-L; \lambda) \quad (9)$$

$$\lambda = \frac{1}{\sigma^2} \left[\sum_{h=1}^{L} \overline{Y_h^2} - \frac{1}{N} \left(\sum_{h=1}^{L} \sqrt{N_h} Y_h \right)^2 \right] \quad (10)$$

where, λ is the non-central parameter; Y_h is the mean value of layer h.

(2) Ecological detector: It is used to confirm whether there is a significant difference between the influences of two independent variables X_1 and X_2 on the spatial distribution of dependent variable Y. The significance is tested by F statistics:

$$F = \frac{N_{X1}(N_{X2}-1)SSW_{X1}}{N_{X2}(N_{X1}-1)SSW_{X2}} \quad (11)$$

$$SSW_{X1} = \sum_{h=1}^{L1} N_h \sigma_h^2, SSW_{X2} = \sum_{h=1}^{L2} N_h \sigma_h^2 \quad (12)$$

where, N_{X1} and N_{X2} respectively represent the sample capacity of two factors X_1 and X_2; SSW_{X1} and SSW_{X1} respectively represent the sum of the intra layer variance of the stratification formed by X_1 and X_2; h is the stratification (classification or partition) of the dependent variable Y or the independent variable X; $L1$ and $L2$ respectively represent the number of variables X_1 and X_2. Where H_0 is assumed to be null hypothesis: $SSW_{X1} = SSW_{X2}$. If H_0 is rejected at the significance level of α, it indicates that there is a significant difference between the two factors X_1 and X_2 on the spatial distribution of attribute Y.

(3) Risk-detector: It judges whether the mean values of attributes are significantly different between two sub-regions. High-risk areas of soil erosion can be identified by t statistics:

$$t_{\overline{y}_{h=1} - \overline{y}_{h=2}} = \frac{\overline{Y}_{h=1} - \overline{Y}_{h=2}}{\left[\frac{Var(\overline{Y}_{h=1})}{n_{h=1}} + \frac{Var(\overline{Y}_{h=2})}{n_{h=2}} \right]^{\frac{1}{2}}} \quad (13)$$

Table 1 P values of different land cover types in the study area

	Land cover type	P values
1	Forest	1
2	Grassland	1
3	Waterbody	0
4	Construction area	0
5	Wasteland	1
6	Paddy field	0.15
7	Dryland	0.4

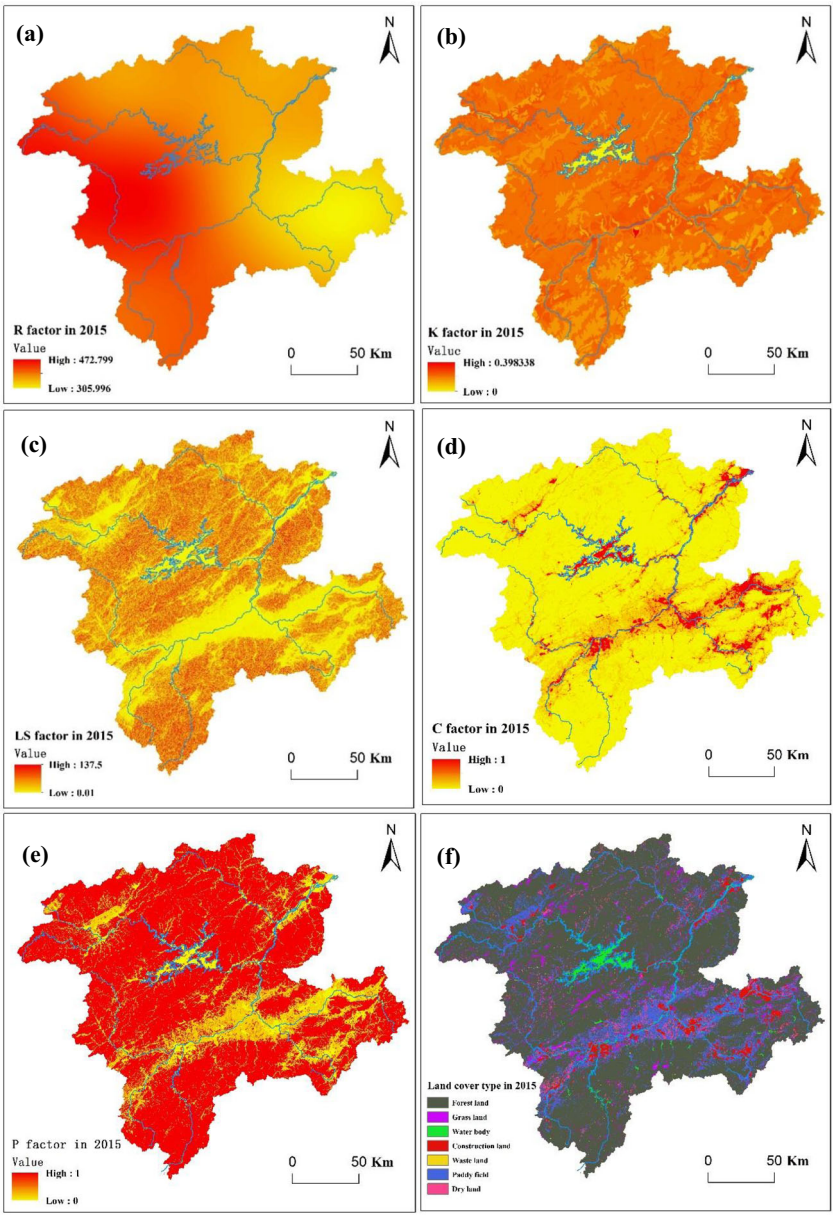

Fig. 2 The map of RUSLE factor including R (**a**), K (**b**), LS (**c**), C (**d**), P (e), and land cover type (**f**)

where, $\overline{Y}_h$ represents the mean value of attributes in stratification h; N_h represents the number of samples in stratification h, and Var represents variance. The statistics t approximately obeys the student's t distribution, where the calculation method of degrees of freedom is:

$$\mathrm{df} = \frac{\dfrac{\mathrm{Var}\left(\overline{Y}_{h=1}\right)}{n_{z=1}} + \dfrac{\mathrm{Var}\left(\overline{Y}_{h=2}\right)}{n_{h=2}}}{\dfrac{1}{n_{h=1}-1}\left[\dfrac{\mathrm{Var}\left(\overline{Y}_{h=1}\right)}{n_{h=1}}\right]^2 + \dfrac{1}{n_{h=2}-1}\left[\dfrac{\mathrm{Var}\left(\overline{Y}_{h=2}\right)}{n_{h=2}}\right]^2} \quad (14)$$

Null hypothesis H_0: $\overline{Y}_{h=1} = \overline{Y}_{h=2}$, if H_0 is rejected under the confidence level α, it is considered that there is a significant difference in the attribute mean between the two sub regions.

(4) Interaction detector: This sub-detector compares the q values (q (X_1) and q (X_2)) to the interaction q value (q ($X_1 \cap X_2$)) to identify their interaction. The relationship can be described by 5 categories: non-linear weakness (q ($X_1 \cap X_2$) < Min(q (X_1), q (X_2))), single-factor non-linear weakness (Min(q (X_1), q (X_2)) < q ($X_1 \cap X_2$) < Max(q (X_1), q (X_2))), two-factor enhancement (q ($X_1 \cap X_2$) > Max(q (X_1), q (X_2))), independent (q ($X_1 \cap X_2$) = q (X_1) + q (X_2)), and non-linear enhancement (q ($X_1 \cap X_2$) > q (X_1) + q (X_2)).

Geographic detectors require category variables as inputs. The discretization method with the highest q value are commonly used (Wang and Xu 2017; Cao et al. 2013). Thus, we set the number of intervals depending on our experience, and the q value was used as an indicator of the effectiveness of discretization methods. Cao et al. (2013) pointed out that the natural breaks (Jenks) was a useful method once the range of intervals was determined, which has been a widely and commonly used method (Jenks 1967; Fischer and Wang 2011). Based on the method proposed by Cao et al. (2013), continuous numerical variables, such as rainfall, elevation, slope, and vegetation coverage, are classified into nine categories from 1 to 9 (Table 2). The driving factors are extracted to 26,309 points by a uniform sampling method of 1 km equidistant grid.

Above all, a linear regression model was adopted to quantify the contribution of annual rainfall erosivity and vegetation coverage to soil rate temporally using the goodness of fit (R^2).

3 Results

3.1 Spatial pattern of soil erosion

The average rate of soil erosion was 1605.82 t km^{-2} year^{-1} with a total 6375.74 × 10^4 t soil erosion at QTC in 2015. Soil erosion mainly happened in mountainous areas in the south and north parts of the catchment. Soil erosion in the central part was less severe than in other regions.

According to the "Standards for classification of soil erosion" proposed by the Ministry of Water Resources of China, the soil erosion rate was classified into six categories from slight to severe soil erosion (Table 3). The area of soil erosion decreased with the increasing rate of soil erosion, and slight soil erosion (i.e., < 500 t km^{-2} year^{-1}) basically dominated the catchment (Fig. 3a), accounting for 75.64% of the total erosion area (Fig. 3b). Moreover, severe soil erosion mainly distributed in northern mountainous areas, southwest, and southeast of QTC. Extreme soil erosion accounted for only 2.36% of the total catchment area, but the amount of soil erosion took up 41.91% of the total.

The rate of soil erosion increased sharply with a slope gradient up to the stratification 3 (12–18°), and increased slowly when the slope gradients were above 18° (Fig. 4a). Moreover, it also increased with elevation within stratification 2 (128–227 m). When elevation exceeded this level, the rate of soil erosion decreased, and it started to increase if elevation exceeded stratification 5 (Fig. 4b). Furthermore, the rate of soil erosion went through a change from increasing to decreasing trend with the increasing vegetation coverage (Fig. 4b), and it was the highest when the vegetation coverage is between stratification 5 and 6 (50–73%).

The rate of soil erosion differed greatly over different land cover types (Table 4). It was the highest in the wasteland (8146.76 t km^{-2} year^{-1}), followed by those in grassland (3657.04 t km^{-2} year^{-1}), forest (1944.57 t km^{-2} year^{-1}), dry land (1305.49 t km^{-2} year^{-1}), and paddy field (305.56 t km^{-2} year^{-1}), respectively.

3.2 Spatial driving factors of soil erosion

According to the results from the factor detector, vegetation coverage had the largest explanatory power of 7.28%, followed by land cover type (2.03%), elevation and slope (1.34%), and soil type (0.31%), and the least explanatory power by rainfall (0.29%) (Table 5). Moreover, the ecological detector suggested that the impact of vegetation coverage on soil erosion was significantly ($p < 0.05$) larger from the other five factors (Table 5).

The interaction between different factors can significantly improve the explanatory power of soil erosion (Table 6). Except for the bilinear mutual enhancement between land cover type and slope, the mutual enhancement of other factors was non-linear. The interaction between slope and vegetation coverage was the dominating factor, with an explanatory

Table 2 Discretization of continuous numerical variables used in this study

Discretization	Five driving factors			
	Elevation (m)	Annual rainfall (mm)	Slope (degree)	Vegetation coverage (%)
1	14–128	1810–1920	0–6	0–9
2	128–227	1920–2041	6–12	9–24
3	227–336	2041–2137	12–18	24–37
4	336–454	2137–2229	18–23	37–50
5	454–583	2229–2335	23–27	50–62
6	583–731	2335–2438	27–33	62–73
7	731–910	2438–2541	33–38	73–82
8	910–1135	2541–2644	38–44	82–91
9	1135–1777	2644–2747	44–74	91–100

Table 3 Classifications of soil erosion rates according to the Ministry of Water Resources in China

Classification	Soil erosion rates (t km^{-2} year^{-1})	Area (km^2)	Mean soil erosion rates (t km^{-2} year^{-1})	Soil loss (10^4 t year^{-1})	Ratio of area (%)	Ratio of annual soil loss/(%)
Slight	< 500	30,031.28	16.77	50.36	75.64	0.79
Light	500–2500	3818.01	1333.09	508.98	9.62	7.98
Moderate	2500–5000	2171.86	3613.61	784.82	5.47	12.31
Intense	5000–8000	1378.24	6344.75	874.46	3.47	13.71
Extreme	8000–150,000	1369.88	10,842.40	1485.28	3.45	23.30
Severe	> 150,000	935.94	28,549.65	2672.06	2.36	41.91

power of 32.69%. The interaction between vegetation coverage and land cover type, elevation reached 23.05% and 23.22%, respectively.

High-risk areas, defined as the regions with relatively high soil erosion rates, were distributed in the regions with land cover type as wasteland, or elevation between 1135 and 1777 m, or vegetation coverage between 50 and 61%, or annual rainfall from 2604 to 2709 mm, or slope 32.51–37.68 or soil type as Yellow-brown earth. There were also significant ($p < 0.05$) differences between two stratifications for elevation and vegetation coverage. Accordingly, the percentage of stratifications with significant differences (PSD) between the two stratifications showed that 86.11% of stratifications were significantly different from others for vegetation coverage and elevation (Table 7).

3.3 Temporal driving factors of soil erosion

Temporally, the rate of soil erosion fluctuated greatly with a slight increase from 1164.63 t km^{-2} year^{-1} in 2007 to 1605.82 t km^{-2} year^{-1} in 2015 (Fig. 5a). The rainfall erosivity also slightly increased from 3850.26 MJ mm ha^{-1} h^{-1} year^{-1} in 2007 to 6559.69 MJ mm ha^{-1} h^{-1} yr^{-1} in 2015. Vegetation coverage increased from 64.59% in 2006 to 67.75% in 2008, remained fluctuating around 67.5%, and finally increased from 67.33% in 2013 to 69.26% in 2015 (Fig. 5b).

To further explore the changing contributions of rainfall, land cover type, and vegetation coverage to the temporal heterogeneity of soil erosion, factor detectors were used to detect soil erosion from 2006 to 2015. The explanatory power of vegetation coverage was always higher than the other five factors ($p < 0.05$), and It went through a transition from an increasing trend to a decreasing trend. The explanatory power of elevation presented a decreasing trend, no obvious changes were detected over the remaining factors (Fig. 6).

The interactive detector was used to detect the temporal variations of interaction between two factors. The explanatory power showed that three combinations with strong interactions in the past 10 years were vegetation coverage with slope, elevation, and land cover type (Fig. 7). The explanatory power of the interaction between vegetation coverage and slope greatly improved from 2006 (23.77%), reached a maximum of 35.17% in 2008, and then fluctuated about 33% in 2009–2015.

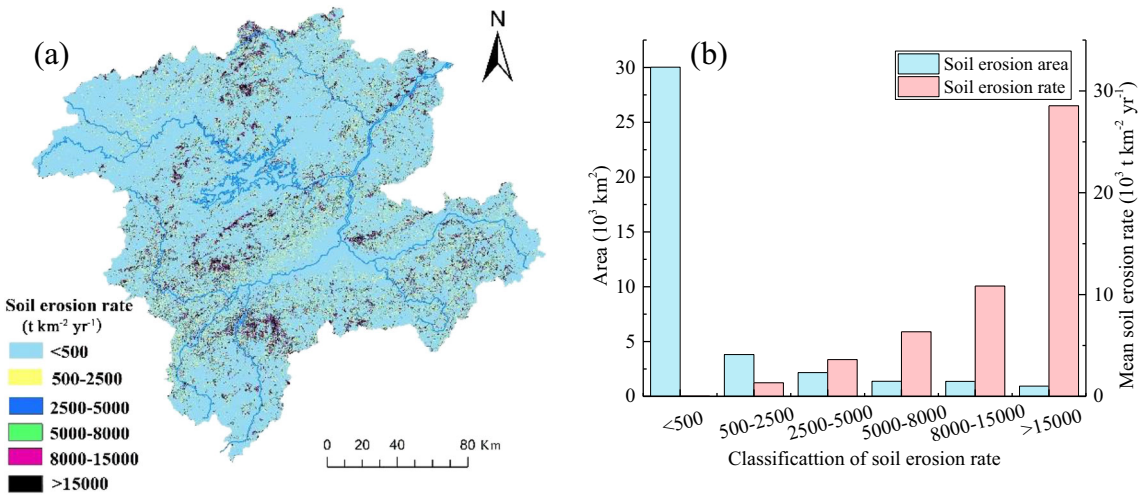

Fig. 3 Spatial distribution of soil erosion rate (**a**) and the corresponding statistics (**b**) in 2015

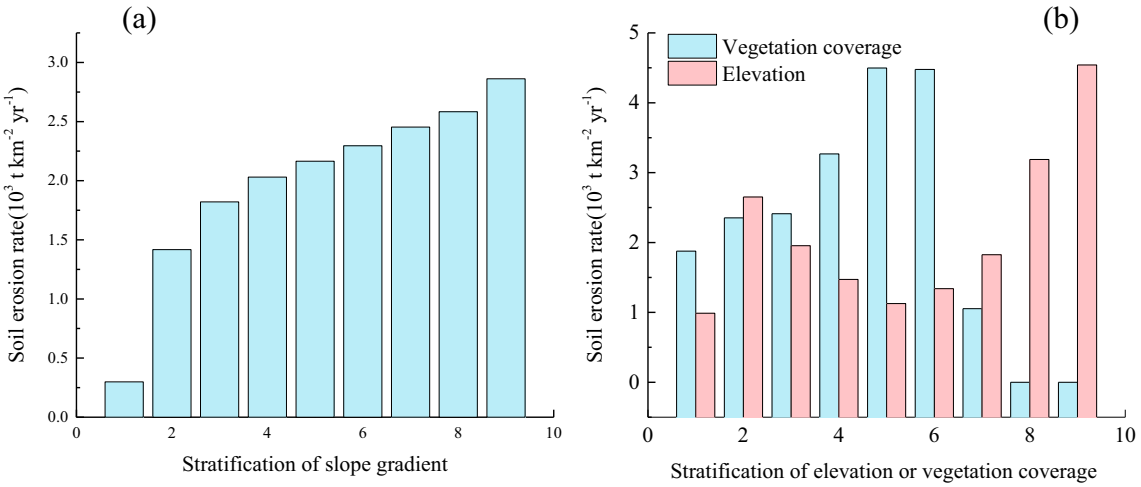

Fig. 4 Soil erosion rate at different slope gradients stratification (**a**) and elevation, vegetation stratification (**b**)

4 Discussions

4.1 Model validation

RUSLE is an empirical model, and it can be challenging to validate it on the watershed scale. But methods used in estimating the RUSLE factors have been used in QTC by other researchers (Zhou et al. 2019) with a similar spatial distribution of soil erosion rate. Besides, we validated the soil erosion rates via sediment delivery ratio (SDR) in the sub-catchment (Lan river). The average SDR was 0.117 from 2006 to 2015, closed to the annual average of 0.132 in Lan river sub-catchment (Li and Liu 2006). Plus, SDR was 0.11 from 1996 to 2005 in QTC (Ministry of Water Resources of China 2010). Therefore, RUSLE should be applicable in QTC.

For further validation, the rate of soil erosion concluded in this study was compared with previous studies. Through a field survey, Liang et al. (2008) proposed an average rate of soil erosion of 3419 t km^{-2} year^{-1} in the hilly region of southern China. Ye and Yang (2007) suggested a rate of soil erosion of 2400 t km^{-2} year^{-1} in Zhejiang province through the field survey. In the hilly region of south Anhui province, Zhao et al. (2016) also obtained a rate of 730 t km^{-2} year^{-1} using RUSLE. The average rate of soil erosion is 1359 t km^{-2} year^{-1} in the study area during 2006–2015, which is within a reasonable range. Differences in data and methods may justify the differences in specific values. Therefore, the rate of soil erosion obtained by RUSLE in this study is reliable.

4.2 Spatial heterogeneity of soil erosion

The simulated soil erosion rate is much higher than the soil loss tolerance (200 t km^{-2} year^{-1}, provided by the Ministry of Water Resources of China) in the hilly region of southern China, and it shows great spatial heterogeneity in QTC influenced by complicated natural and anthropogenic factors (e.g., slope, elevation, and land use type, etc.). Soil erosion rate differed considerably over different land cover types in this study. Higher rates of soil erosion over forest and grassland are consistent with Yang et al.' s conclusion (2017). Moreover, Wu et al. (2016) suggested that the rates of soil erosion with 60%, 80%, and 90% vegetation coverage at 15° runoff plots were 2433 t km^{-2} year^{-1}, 2179 t km^{-2} year^{-1}, and 2054 t km^{-2} year^{-1}, respectively. Therefore, rate of soil erosion over forest (1944.57 t km^{-2} year^{-1}) in this study should be reliable. The severe soil erosion over forest lies in the fact that forest is mainly distributed in those steep areas. Soil erosion increases sharply in areas with slope gradients below 18°, which is highly related to vegetation pattern. Vegetation is

Table 4 Soil erosion rates over different land cover types

Land cover types	Area/ km^{-2}	Soil erosion rate/t km^{-2} year^{-1}	Soil erosion amount/ 10^4 t year^{-1}	Area ratio/%	Annual soil erosion ratio/%
Forest	28,683.17	1944.57	5577.64	72.24	87.35
Grassland	1232.29	3657.04	450.65	3.10	7.06
Wasteland	12.74	8146.76	10.38	0.03	0.16
Paddy field	5886.53	305.56	179.87	14.83	2.82
Dryland	1276.24	1305.49	166.61	3.21	2.61

Table 5 The explanatory power of each driving factor derived from geographic detectors

	Land cover type	Elevation	Vegetation coverage	Annual rainfall	Slope	Soil type
Explanatory	2.03%	1.34%	*7.28%*	0.22%	1.34%	0.31%
Elevation	N					
Vegetation coverage	Y	Y				
Annual rainfall	Y	N	Y			
Slope	N	N	Y	N		
Soil type	Y	N	Y	N	N	

All results were tested at 95% significant level. "Y" denotes a significant interaction and "N" otherwise

mostly distributed in mountainous areas with flat slope gradients and the plain is mainly occupied by arable land.

Soil erosion is likely to happen in regions with vegetation coverage from 50 to 73%, which agrees with findings in previous studies (e.g., Wang et al. 2013; Gao et al. 2018). On the one hand, areas with less than 50% vegetation coverage in QTC are mostly plain areas with the primary land cover type as paddy field and construction land, which have small rates of soil erosion. On the other hand, soil erosion may be affected by the thickness of the available erodible soil layer (Kim et al. 2016; Gao et al. 2018). When the vegetation coverage is below 50%, the available eroded soil layer is thin and the amount of erosion is small. With increasing vegetation coverage, the available eroded soil layer becomes thicker and the amount of soil erosion increases accordingly. When the vegetation coverage exceeds 73%, it can effectively prevent soil erosion. This highlights the significant interaction between vegetation coverage and slope, as well as that between land cover type and elevation.

Soil erosion increases with an increasing elevation between stratification 1–2 and 5–9. However, in areas with elevation falling in stratification 3–4, the rate of soil erosion decreases (Fig. 4b). As shown in Fig. 8, the slope gradient and vegetation coverage increase with increasing elevation since vegetation coverage is relatively small at the low-elevation areas but decreases when elevation exceeds stratification 5, and the slope gradient always increases with elevation.

4.3 Spatial analysis on driving factors of soil erosion heterogeneity

In this study, the impacts of six driving factors including annual rainfall, land cover type, slope, elevation, vegetation coverage, and soil type, as well as their interaction on soil erosion were quantified. Wang et al. (2018) showed that land cover type could explain 68.5% of the spatial distribution of soil erosion in southwestern China. However, in our study, single factor alone cannot explain much variability in soil erosion. In QTC, vegetation coverage had the highest explanatory power (7.28%). This may be caused by the steep slope, abundant annual precipitation, and relatively luxuriant vegetation in QTC. The complex interactions among these factors can hardly be justified by one single factor. Moreover, vegetation can intercept rainfall and slow down runoff, which further reduces runoff and sediment yield (Liu et al. 2015). Therefore, the interaction between slope and vegetation coverage is the dominating factor. Areas with steep slopes and small vegetation coverage suffer from severe soil erosion, which is in urgent need of reasonable land use regulation.

The risk detector showed that 86.11% of stratifications had a significant difference within vegetation coverage and elevation stratifications. In the study area, higher elevation corresponds to larger slope gradient, and the vegetation coverage first increases and then decreases with increasing elevation. Therefore, the lower vegetation cover and higher slope

Table 6 The explanatory power of the interactions among different driving factors in soil erosion

Driving factors	Land cover type	Elevation	Vegetation coverage	Annual rainfall	Slope	Soil type
Land cover type	2.03%					
Elevation	3.65%	1.34%				
Vegetation coverage	*23.05%*	*23.22%*	7.28%			
Annual rainfall	2.51%	2.25%	8.86%	0.22%		
Slope	2.49%	3.58%	*32.69%*	2.06%	1.34%	
Soil type	2.9%	2.08%	12.91%	0.98%	2.81%	0.31%

Table 7 Soil erosion rates (t km^{-2} a^{-1}) and high-risk areas, and the percentage of stratification with significant difference (PSD) for each driving factor

Driving factors	High-risk areas	Mean soil erosion	PSD
Land cover type	Waste land	8146.76	66.66%
Elevation	1135–1777	5555.38	*86.11%*
Vegetation coverage	50–62%	4995.39	*86.11%*
Annual rainfall	2644–2747	1922.45	55.56%
Slope	33–38	2453.61	44.44%
Soil type	Yellow-brown earths	4947.21	54.55%

gradient in 1355–1777 had a higher soil erosion rate. In addition, the lower vegetation coverage range of 50–60% also induced in a higher soil erosion rate (Fig. 9). Therefore, more attention should be directed to regions with an elevation between 1135 and 1777 m or vegetation coverage between 50 and 62%. The results indicated that it also suggests that stratification can well reflect the differences in soil erosion in different stratifications, which is largely due to the considerable elevation difference since the stratification of elevation reflects differences in climate, topography, and vertical dynamic of vegetation.

4.4 Temporal analysis on driving factors of soil erosion heterogeneity

For the period of 2006–2015, factors such as geomorphology and soil properties can be regarded as constant, whereas changes in land cover type, vegetation coverage, and rainfall can be relatively drastic. Therefore, they should be taken into account when the driving factors of the temporal variations of soil erosion are discussed.

A slight increase in soil erosion occurred in QTC from 2006 to 2015 (Fig. 5a) with a significant relationship between annual rainfall erosivity and soil erosion rate (Fig. 5b; R^2 =

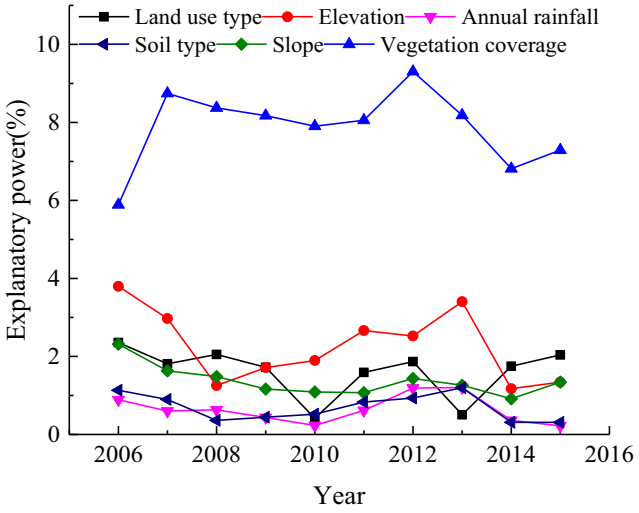

Fig. 6 Temporal variations of explanatory power of each driving factor during 2006–2015

0.60). However, if the rainfall erosivity was assumed to be constant, soil erosion showed a significant decreasing trend. This could be attributed to the enhanced soil protection by vegetation restoration since annual rainfall erosivity and vegetation coverage can temporally explain 60% and 32% of soil erosion.

Moreover, conversions among different land cover types were common in QTC (Table 8), mainly from paddy field to construction land or water body, from forest to grassland or water body, and from dry land to construction land. These land cover changes are beneficial for reducing soil erosion, still, they are insufficient to offset the erosion caused by rainfall.

Temporal variation in the explanatory power of vegetation coverage is different from the other five factors (Fig. 6). The average vegetation coverage has increased in areas with elevation less than 583 m but decreased in areas with an elevation between 1135 and 1777 m from 2006 to 2015 (Table 9). The soil erosion rate decreases at low and middle altitudes and

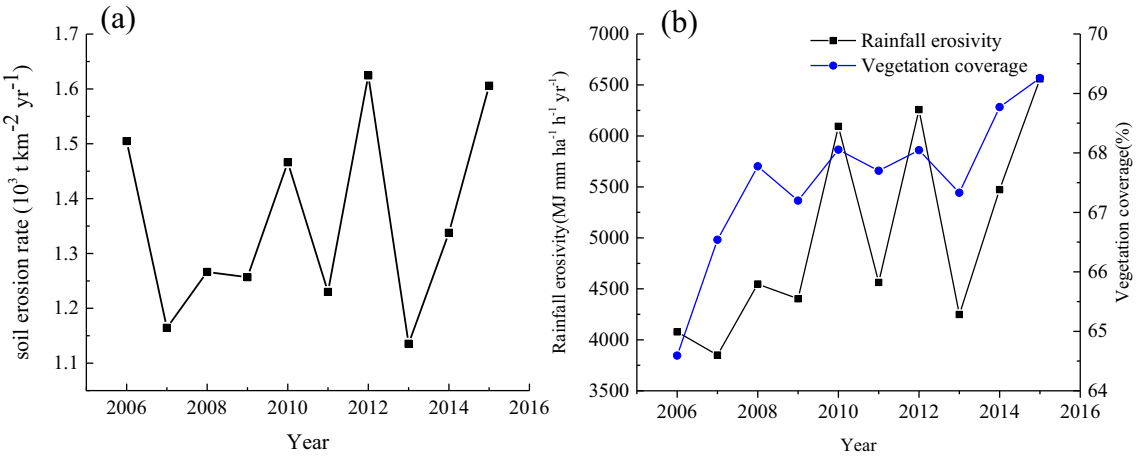

Fig. 5 Temporal variation of soil erosion rate (**a**) and vegetation coverage, rainfall erosivity (**b**)

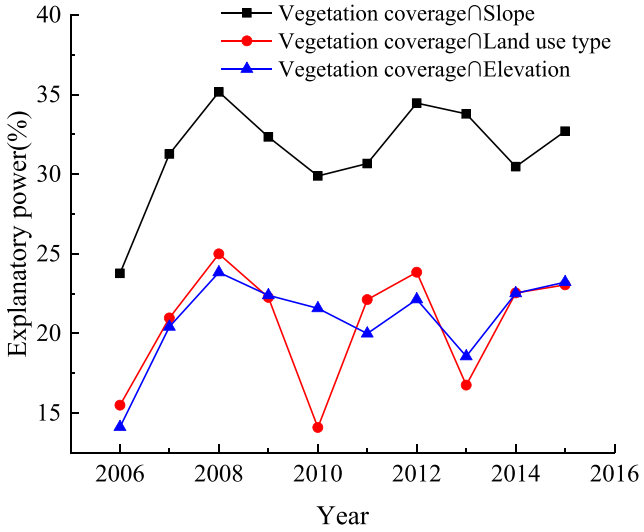

Fig. 7 Temporal variations of explanatory power of interaction among different driving factors

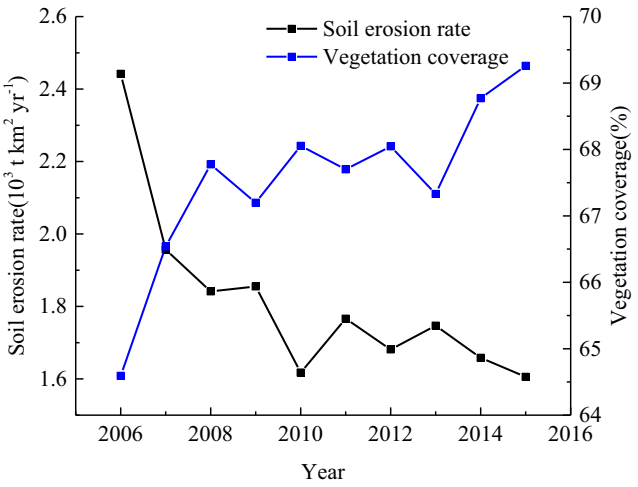

Fig. 9 Temporal variations of soil erosion rate with vegetation coverage when rainfall erosivity is assumed constant in 2015

increased at high altitudes, which enhances the explanatory power of elevation to soil erosion but weakens the explanatory power of vegetation coverage. Therefore, the explanatory power of elevation to soil erosion varies from decrease to increase during 2006–2015. Impacted by the interaction between elevation and vegetation coverage, there is a threshold in annual average vegetation coverage. Above the threshold, the explanatory power of each factor to soil erosion will not decrease with increasing vegetation coverage. Figure 9 presented a decreasing trend in soil erosion rate with increasing vegetation coverage when the rainfall erosivity is assumed constant. When vegetation coverage reaches 68%, the decrease in the amount of soil erosion slows down. Therefore, vegetation coverage in high-altitude QTC should be increased in the future to reduce soil erosion.

In addition, given the relationship between slope and elevation (Fig. 8), interaction between vegetation coverage and elevation is similar. The interaction between vegetation coverage and land cover type shows a small upward trend during 2006–2015, probably due to the conversion of paddy field and forest to construction land and grassland. In this study, soil erosion over construction land is not considered, so land cover change is generally beneficial to conserve soil and water. On the other hand, the plain areas are featured by small vegetation coverage and vulnerable land cover type (e.g., dry land), and rate of soil erosion differs slightly, resulting in the weak explanatory power of the selected factors.

4.5 Uncertainty analysis

Thin soil layers tend to cause the outcrop of bedrocks in the hilly region. Therefore, soil erosion rate might be overestimated for the wasteland. Meanwhile, the gully erosion and gravity erosion were not considered in the RUSLE, which may bring in certain underestimation of soil erosion rate. The modle could be modified to suit the hilly region in the future.

Moreover, selecting a desirable discretization method can be challenging in the application of geographic detectors (Cao

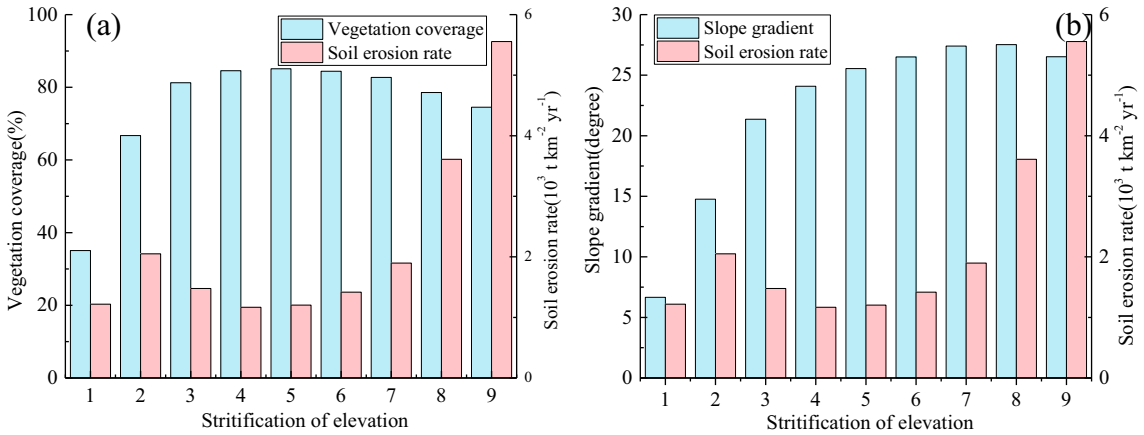

Fig. 8 Change of soil erosion with different elevation and vegetation coverage (**a**) and change of slope and vegetation coverage with elevation (**b**)

Table 8 Land use transition matrix from 2006 to 2015 (km^2)

2015, 2006	Forest	Grassland	Waterbody	Construction	Wasteland	Paddy field	Dryland	Total area 2006
Forest	26,211.57	413.44	184.09	247.62	8.61	1402.18	377.71	28,845.22
Grassland	354.75	707.27	5.42	19.45	0.77	61.05	15.68	1164.39
Waterbody	206.77	6.59	643.51	40.10	0.02	123.58	30.46	1051.03
Construction	80.72	5.75	21.61	638.60	0.17	179.70	29.08	955.64
Wasteland	4.48	0.06	0.01	0.27	2.53	0.39	0.52	8.26
Paddy field	1444.66	76.69	111.03	626.13	0.54	3888.18	285.56	6432.79
Dryland	351.43	19.45	23.41	98.91	0.10	230.52	536.90	1260.71
Total area 2015	28,654.39	1229.25	989.08	1671.07	12.73	5885.61	1275.91	39,718.04

et al. 2013), which is beyond the scope of this study and needs further research. Although the substantial impact of different discretization methods on the results by geographic detectors was not discussed in this study, the discretization method with the largest q value we adopted has been used in previous studies (Wang and Xu 2017; Cao et al. 2013). The results should be regionally optimal and meaningful.

Although the specific value of the explanatory power could be slightly different with different discretization methods, the explanatory power reveals a reliable comparison of the relative contribution of each driving factor or the interaction between two driving factors, Therefore, this study can still provide a meaningful reference for future soil erosion control measures in the study area.

5 Conclusions

Based on RUSLE and geographic detectors, driving factors of soil erosion were quantified spatiotemporally in QTC, southeastern China, from 2006 to 2015. Major conclusions are as follows:

(1) The explanatory powers of six driving factors to soil erosion are significantly different with the maximum explanatory power of 7.28% by vegetation coverage.

(2) Interaction between these factors can enhance the explanatory power of soil erosion, and the interactive explanatory power of vegetation coverage and slope is 32.69%, and that of vegetation coverage and elevation, vegetation coverage and land cover type reach 23.22% and 23.05%, respectively. High-risk areas are those areas with an elevation between 1135 and 1777 m or vegetation coverage of 50–62%. Therefore, areas with small vegetation coverage and high elevation call for implement of soil and water conservation measures.

(3) Vegetation coverage and its interaction with slope, elevation, and land cover type are the dominating factors in soil erosion during 2006–2015. The increasing explanatory power is mainly caused by the changing vegetation coverage and its spatial distribution. Increasing vegetation coverage in high-altitude areas can effectively protect the soils in the future.

Table 9 Changes of vegetation coverage (%) at different elevations during 2006–2015

Stratification, Year	1	2	3	4	5	6	7	8	9
2006	29.71	57.2	72.32	78.88	82.97	85.57	87.12	86.07	84.75
2007	30.58	60.39	75.57	81.36	84.68	86.69	87.63	86.25	84.28
2008	32.82	64.4	79.09	82.98	83.87	83.86	83.19	80.46	80.99
2009	32.28	62.28	77.59	82.31	84.12	84.88	85.01	82.62	80.86
2010	33.48	62.92	78.48	83.33	85.39	86.14	85.63	81.73	77.79
2011	31.97	61.96	77.7	83.25	85.66	86.67	86.95	84.47	81.56
2012	32.75	62.52	78.67	83.86	85.95	86.48	85.92	82.32	77.69
2013	30.42	60.26	76.45	82.74	86.25	88.35	89.64	88.5	86.63
2014	33.61	65.28	80.06	84.19	85.32	85.24	84.46	81.71	78.07
2015	35.08	66.7	81.25	84.57	85.09	84.41	82.73	78.55	74.51

Acknowledgements This work was financially supported by the project of the National Natural Science Foundation of China (grant number 41977066).

References

Borrelli P, Robinson DA, Fleischer LR, Lugato E, Ballabio C, Alewell C, Meusburger K, Modugno S, Schütt B, Ferro V, Bagarello V, Oost KV, Montanarella L, Panagos P (2017) An assessment of the global impact of 21st century land use change on soil erosion. Nat Commun 8(1):2013

Borrelli P, Van Oost K, Meusburger K, Alewell C, Lugato E, Panagos P (2018) A step towards a holistic assessment of soil degradation in Europe: coupling on-site erosion with sediment transfer and carbon fluxes. Environ Res 161:291–298

Cai CF, Ding SW, Shi ZH, Huang L, Zhang GY (2000) Study of applying USLE and geographical information system IDRISI to predict soil erosion in small watershed. J Soil Water Conserv 14(2):19–24

Cao F, Ge Y, Wang JF (2013) Optimal discretization for geographical detectors-based risk assessment. GISci Remote Sens 50(1):78–92

Chen SX, Yang XH, Xiao LL, Cai HY (2014) Study of soil erosion in the southern hillside area of China based on RUSLE model. Resour Sci 36(6):1288–1297

El Kateb H, Zhang H, Zhang P, Mosandl R (2013) Soil erosion and surface runoff on different vegetation covers and slope gradients: a field experiment in Southern Shaanxi Province, China. Catena 105: 1–10

Feng T, Wei W, Chen L, Rodrigo-Comino J, Die C, Feng X, Ren K, Brevik EC, Yu Y (2018) Assessment of the impact of different vegetation patterns on soil erosion processes on semiarid loess slopes. Earth Surf Proc Land 43(9):1860–1870

Fischer MM and Wang JF (2011) Spatial data analysis: models, methods and techniques, 82.Berlin: Springer

Gao JB, Wang H, Zuo L (2018) Spatial gradient and quantitative attribution of karst soil erosion in Southwest China. Enviro Monit Assess 190(12):730

Golosov V, Yermolaev O, Litvin L, Chizhikova N, Kiryukhina Z, Safina G (2018) Influence of climate and land use changes on recent trends of soil erosion rates within the Russian Plain. Land Degrad Dev 29(8):2658–2667

Huang JL, Hong HS, Zhang LP, Du P (2004) Study on predicting soil erosion in Jiulong River watershed based on GIS and USLE. J Soil Water Conserv 18(5):75–79

Jenks GF (1967) The data model concept in statistical mapping. International Yearbook Cartography 7:186–190

Jiang L, Bian JH, Li AN, Lei GB, Nan X, Feng WL, Li G (2014) Spatial-temporal changes of soil erosion in the upper reaches of Minjiang River from 2000 to 1000. J Soil Water Conserv 28(01):18-25+35

Khan M, Gong Y, Hu T, Lal R, Zheng J, Justine M, Azhar M, Che M, Zhang H (2016) Effect of slope, rainfall intensity and mulch on erosion and infiltration under simulated rain on purple soil of South-Western Sichuan province, China. Water 8(11):528

Kim J, Ivanov VY, Fatichi S (2016) Environmental stochasticity controls soil erosion variability. Sci Rep-UK 6:22065

Kinnell PIA (2010) Event soil loss runoff and the universal soil loss equation family of models: a review. J Hydrol 385(1–4):384–397

Lal R (1998) Soil erosion impact on agronomic productivity and environment quality. Crit Rev Plant Sci 17(4):319–464

Li ZG, Liu BZ (2006) Calculation on soil erosion amount of main river basin in China. Sci Soil Water Conserv 4(2):1–6

Liang Y, Zhang B, Pan XZ (2008) Current status and comprehensive control strategies of soil erosion for hilly region in the Southern China. Sci Soil Water Conserv 6(1):22–27

Liu BY, Nearing MA, Risse LM (1994) Slope gradient effects on soil loss for steep slopes. T ASAE 37(6):1835–1840

Liu BY, Nearing MA, Shi PJ, Jia ZW (2000) Slope length effects on soil loss for steep slopes. Soil Sci Soc Am J 64(5):1759–1763

Liu XY, Yang ST, Li XY, Zhou X, Luo Y, Dang SZ (2015) The current vegetation restoration effect and its influence mechanism on the sediment and runoff yield in severe erosion area of Yellow River Basin. Sci Sini Technol 45(10):1052

Mhaske SN, Pathak K, Basak A (2019) A comprehensive design of rainfall simulator for the assessment of soil erosion in the laboratory. Catena 172:408–420

Ministry of Water Resources of China (2007) SL190-2007 standards for classification and gradation of soil Erosion. Beijing: China Water Power Press 2007

Ministry of Water Resources of China (2010) Prevention and control of soil and water loss and ecological security in China. Science Press, Beijing

Rao E, Ouyang Z, Yu X, Xiao Y (2014) Spatial patterns and impacts of soil conservation service in China. Geomorphology 207:64–70

Ren Y, Deng LY, Zuo SD, Song XD, Liao YL, Xu CD, Chen Q, Hua LZ, Li ZW (2016) Quantifying the influences of various ecological factors on land surface temperature of urban forests. Environ Pollut 216:519–529

Sharpley AN, Williams JY (1990) EPIC-erosion/productivity impact calculator: 1, Model Documentation. USDA Techn Bull 1759:235

Shi ZH, Ai L, Li X, Huang XD, Wu GL, Liao W (2013) Partial least-squares regression for linking land-cover patterns to soil erosion and sediment yield in watersheds. J Hydrol 498:165–176

Siswanto SY, Francés F (2019) How land use/land cover changes can affect water, flooding and sedimentation in a tropical watershed: a case study using distributed modeling in the Upper Citarum watershed, Indonesia. Environ Earth Sci 78:550

Sun W, Shao Q, Liu J, Zhai J (2014) Assessing the effects of land use and topography on soil erosion on the Loess Plateau in China. Catena 121:151–163

Wang JF, Xu CD (2017) Geodetector: principal and prospective. Acta Geograph Sin 72(1):116–134

Wang JF, Li XH, Christakos G, Liao YL, Zhang T, Gu X, Zheng XY (2010) Geographical detectors-based health risk assessment and its application in the neural tube defects study of the Heshun region, China. Int J Geogr Inf Sci 24(1):107–127

Wang Y, Cai YL, Pan M (2013) Analysis on relationship between soil erosion and land use in Wujiang River Basin in Guizhou Province. Res Soi Water Conserv 20(3):11–18

Wang H, Gao JB, Hou WJ (2018) Quantitative attribution analysis of soil erosion in different morphology types of geomorphology in karst areas: based on the geographic detector method. Acta Geograph Sin 73(9):1674–1686

Wei W, Chen LD, Fu BJ, Lu YH, Gong J (2009) Responses of water erosion to rainfall extremes and vegetation types in a loess semiarid hilly area, NW China. Hydrol Process 23:1780–1791

Wei W, Chen LD, Yang L, Fu BJ, Sun RH (2012) Spatial scale effects of water erosion dynamics: complexities, variabilities, and uncertainties. Chin Geogr Sci 22(2):127–143

Wu GY, Jin WP, Zhong X, Liu CQ, Liu SB, Zheng EH (2016) Initial study on the impact of vegetation coverage to soil Erosion in red soil areas of South China. Subtropical Soil Water Conserv 28(4):1–4

Xu H, Li Z, Lin J, Jiang A (2016) Influences of rainfall and underlying surface conditions on soil erosion and sediment yield in Yanshan Rocky Mountain area. J Mountain Sci 34(1):46–53

Yang R, Xu Q, Long H (2016) Spatial distribution characteristics and optimized reconstruction analysis of China's rural settlements during the process of rapid urbanization. J Rural Stud 47:413–424

Ye YQ, Yang X (2007) Temporal and spatial change of soil and water loss in Zhejiang Province. Soils 39(3):400–403

Yu Y, Wei W, Chen L, Feng T, Daryanto S (2019) Quantifying the effects of precipitation, vegetation, and land preparation techniques on runoff and soil erosion in a loess watershed of China. Sci Total Environ 652:755–764

Zha LS, Deng GH, Gu JC (2015) Dynamic changes of soil erosion in the Chaohu Watershed from 1992 to 2013. Acta Geograph Sin 70(11): 1708–1719

Zhang WB, Fu JS (2003) Rainfall erosivity estimation under different rainfall amount. Resour Sci 25(1):35–41

Zhao MS, Li DC, Zhang GL, Cheng XF (2016) Evaluation of soil erosion and soil nutrient loss in Anhui Province based on RUSLE model J. Acat Pedol Sin 53(1):28–38

Zhou FJ, Chen MH, Lin FX, Huang YH, Lu CL (1995) The rainfall erosivity in Fujian Province. J Soil Water Conserv 9(1):13–18

Zhou MM, Deng J, Lin Y, Belete M, Wang K, Comber A, W K, Gan M (2019) Identifying the effects of land use change on sediment export: integrating sediment source and sediment delivery in the Qiantang River Basin, China. Sci Total Environ 686: 38–49

Zhu SX, Gong J, Lin EB, Jin SL (2013) Characteristics of under forest soil and water loss in hilly areas of South China and its control measures. Subtropical Soil Water Conserv 25(3):24–30